Effect of surfactant concentration on the stacking modes of organo-silylated layered double hydroxides

Qi Tao [a,b,c], Jie Yuan [d], Ray L. Frost [b,*], Hongping He [a,b,*], Peng Yuan [a], Jianxi Zhu [a]

[a] *Guangzhou Institute of Geochemistry, Chinese Academy of Sciences, Guangzhou 510640, PR China*
[b] *Inorganic Materials Research Program, School of Physical and Chemical Sciences, Queensland University of Technology, GPO Box 2434, Brisbane, Queensland 4001, Australia*
[c] *Graduate School of Chinese Academy of Sciences, Beijing 100039, PR China*
[d] *Medical College, Jinan University, Guangzhou 510632, PR China*

ARTICLE INFO

ABSTRACT

The effects of the surfactant concentration on the structure, morphology and thermal property of silylated hydrotalcites have been investigated. By in-situ coprecipitation, the surfaces of layered double hydroxides (LDHs) have been modified by using 3-aminopropyltriethoxysilane (APTS) and anionic surfactant, Na-dodecylsulfate (SDS). Two different stacking modes in the resultant materials were detected by X-ray diffraction (XRD). One has an identical structure of LDHs, in which the SDS and APTS only bond to the outside surfaces and plate edges of LDH. The other is with enlarged interlayer distance, in which SDS and APTS combined with the inside surfaces of LDH. With the increased loading of SDS and APTS, the surface of the modified LDH appeared rough as observed in the transmission electron microscopy (TEM) images. The attenuated total reflection Fourier-transform infrared (ATR FTIR) spectra of the silylated hydrotalcites showed a series of bands attributed to –NH$_2$ and Si–O–M (M = Mg and Al), proving that APTS has successfully been grafted onto LDH. The thermogravimetric curves (TG) showed that the silane grafted samples have less –OH concentration and less interlayer water, as a result of the –OH consumption during the condensation reaction between Si–OH and –OH on LDH surface. These nanomaterials are of potential applications including clay-based nanocomposites, adsorbents for removal of organic contaminants from water and flame retardant materials.

© 2009 Elsevier B.V. All rights reserved.

1. Introduction

Novel materials may be obtained by the simple modification of the surfaces. One method is to silylate the surfaces of clay minerals such as kaolinite, montmorillonite and layered double hydroxides. As "coupling agents", organo-functionalized silanes have been proven effective in enhancing the adhesion of polymers to inorganic substrates, especially in the presence of water (Ingall et al., 1999; Angloher et al., 2007; Lee et al., 2007; Oh et al., 2007; Yeon et al., 2008). This property makes these materials extensively applied in surface modification. Organo-functionalized silanes permit a precise control over the surface component and pore features for specific applications, and at the same time stabilizing the materials against hydrolysis. The products of such chemistry form the basis of novel inorganic–organic hybrid materials, in which the inorganic parts provide mechanical, thermal, and structural stability, whereas the organic parts can change the flexibility of the framework, optical properties and hydrophilic and hydrophobic properties (Zhu et al., 2008).

Layered double hydroxides (LDHs), also known as hydrotalcite-like compounds, are layered clay minerals with a general formula $[M^{2+}_{1-x}M^{3+}_x(OH)_2]^{x+}A^{n-}_{x/n}\cdot mH_2O$, where M^{2+} and M^{3+} are divalent and trivalent cations that occupy octahedral positions in the hydroxide layers, A^{n-} is an interlayer anion and x is defined as the $M^{3+}/(M^{2+} + M^{3+})$ ratio. The excellent anionic exchange capacity makes them potential materials for adsorbents, ion exchangers, pharmaceutics, catalysts or catalyst supports etc (Dimotakis and Pinnavaia, 1990; Cavani et al., 1991; Hermosin et al., 1996; Choudary et al., 2002; You et al., 2002a; Hutson et al., 2004; Domingo et al., 2006). Although, there are many studies on the silylation of the surfaces of clay minerals, for example smectites, very limited attention (Park et al., 2005; Wypych et al., 2005) has been paid to apply this method to the LDHs considering the higher surface charge density (about one positive charge per 25 Å^2 for the case of $x = 0.32$) (Li et al., 2004) when compared with cationic clays. An improved approach is to introduce long carbon chain anions into interlayer space of LDHs, which can not only enlarge the interlayer space but also change the surface property of the LDHs from hydrophilicity to hydrophobicity (Zhu et al., 2008). As a result, the organo molecules with functional groups may be intercalated to react with the hydroxyl groups on the solid surface. Grafting LDHs with 3-aminopropyltriethoxysilane (APTS) was attempted very recently (Park et al., 2005; Wypych et al., 2005), in

* Corresponding authors. He is to be contacted at Guangzhou Institute of Geochemistry, Chinese Academy of Sciences, Guangzhou 510640, PR China.
E-mail addresses: r.frost@qut.edu.au (R.L. Frost), hehp@gig.ac.cn (H. He).

which the dodecylsulfate anion (DS⁻) interlayered LDH was prepared, followed by reacting with APTS in nonaqueous solvents.

The surfactant plays an important role on the synthesis of functionalized materials including surface silylation. Modification of materials with surfactant results in a surface property change of the solid materials from hydrophilicity toward hydrophobicity (Zhu et al., 2008) and displacement of the interlayer anions to form organo-clays with enlarged interlayer spaces (Drezdzon, 1988; Clearfield et al., 1991). The surfactant interlayered LDHs can even lead to exfoliation to form monolayer nanocomposites (Adachi-Pagano et al., 2000; Leroux et al., 2001), which is nearly impossible to happen in the inorganic anions interlayered LDHs.

In this research, we present an in-situ grafting (Zhu et al., 2008) of APTS onto the surface of LDHs in aqueous solution with the assistance of anionic surfactant, Na-dodecylsulfate (SDS). To reveal the roles of the surfactants during silylation procedure, a range of surfactant concentrations was used to synthesize silane grafted LDHs (LDH-Sil) by coprecipitation at a fixed concentration of APTS. The composition, morphology and thermal property of the obtained LDH materials and the conformation of the organic molecules were characterized by X-ray diffraction (XRD), attenuated total reflection Fourier-transform infrared spectroscopy (ATR FTIR), Raman spectroscopy, thermogravimetric analysis (TG), transmission electron microscopy (TEM) and Energy Dispersive X-ray Spectroscopy (EDX).

2. Experimental

2.1. Synthesis of materials

2.1.1. $Mg_6Al_2(OH)_{16}CO_3 \cdot 4H_2O$ (LDH)

The LDHs were prepared by coprecipitation as described previously (Tao et al., 2009). About 9.6 g of $Mg(NO_3)_2 \cdot 6H_2O$ (0.038 mol) and 4.7 g of $Al(NO_3)_3 \cdot 9H_2O$ (0.013 mol) with a molar ratio of 3:1 (Mg^{2+}/Al^{3+}) were dissolved in 90 cm³ distilled water (referred as Solution A). About 4 g NaOH (0.01 mol) was dissolved in 50 cm³ of distilled water (referred as Solution B). Solution B and Solution A were dropped into 50 cm³ distilled water with vigorous stirring. The pH value of the mixture was kept at around 10. The mixture was aged at 80 °C for 12 h. The resultant precipitate was filtered, washed with distilled water, and dried at 80 °C. The obtained material was denoted as LDH.

2.1.2. LDH-SDS-APTS (LDH-Sil)

19.2 g of $Mg(NO_3)_2 \cdot 6H_2O$ (0.075 mol) and 9.4 g of $Al(NO_3)_3 \cdot 9H_2O$ (0.025 mol) with a molar ratio of 3:1 (Mg^{2+}/Al^{3+}) were dissolved in 90 cm³ of distilled water (Solution C). About 8 g NaOH (0.02 mol) together with 0.7, 1.4, 2.2, 2.9, 4.3 and 5.6 g SDS (0.0025, 0.0050, 0.010, 0.015 and 0.020 mol) were dissolved in 50 cm³ distilled water respectively (Solution D). About 5.0 cm³ APTS (0.021 mol) was dissolved in 50 cm³ ethanol (Solution E). At room temperature, solutions C, D and E were dropped to 100 cm³ distilled water with vigorous stirring, maintaining the pH value of the mixture at around 10. The mixture was aged at 80 °C in a water bath for about 12 h, and afterwards, the resultant slurry was filtered, washed with distilled water, and dried at 80 ºC. The obtained materials were denoted as LDH-Sil$_n$ (n stands for the relative content of SDS). For example, when the content of SDS was 0.010 mol, the sample was denoted as LDH-Sil$_{10}$.

2.2. Characterization of materials

2.2.1. X-ray-diffraction

Powder XRD patterns were recorded using a Philips PANalytical X'Pert PRO X-ray diffractometer (radius: 240.0 mm). Incident X-ray radiation was produced from a line focused PW 3373/10 Cu X-ray tube, operating at 40 kV and 40 mA, providing a $K\alpha_1$ wavelength of 1.5418 Å. The incident beam was monochromated through a 0.020 mm Ni filter then passed through a 0.04 rad Soller slit, a

15 mm fixed mask with 0.25° divergence slit, and a 0.5° anti-scatter slit, between 9 and 75° (2θ) at a step size of 0.0167°. For XRD at low angle section, it was between 2 and 10° (2θ) at a step size of 0.0167° with variable divergence slit and 0.125° anti-scatter slit.

2.2.2. Transmission electron microscopy

Transmission electron microscopy (TEM) images were obtained in a Philips CM120 electron microscope operating at an acceleration voltage of 120 kV. The specimens for TEM observation were prepared by the following procedure. The sample was ultrasonically dispersed in ethanol for 5 min, and then a drop of sample suspension was dropped onto a carbon-coated copper grid, which was left to stand for 10 min and transferred into the microscope. The contents of Mg, Al and Si were measured by Energy Dispersive X-ray Spectroscopy (EDX).

2.2.3. Infrared spectroscopy

Infrared spectra were obtained using a Nicolet Nexus 870 FTIR spectrometer with a smart endurance single bounce diamond ATR cell. Spectra over the 4000 to 525 cm⁻¹ range were obtained by the co-addition of 64 scans with a resolution of 4 cm⁻¹ and a mirror velocity of 0.6329 cm s⁻¹.

Spectroscopic band component analysis was undertaken using the Jandel 'Peakfit' software package, which enabled the type of fitting function to be selected and allows specific parameters to be fixed or varied accordingly. Band fitting was done using a Gauss–Lorentz, cross-product function with the minimum number of component bands used for the fitting process. The Gauss–Lorentz ratio was maintained at values greater than 0.7 and fitting was undertaken until reproducible results were obtained with squared correlations (r^2) greater than 0.995.

2.2.4. Thermal analysis

Thermogravimetric analyses and differential thermogravimetric analyses (TG) of samples were recorded on a TG Q500 high-resolution
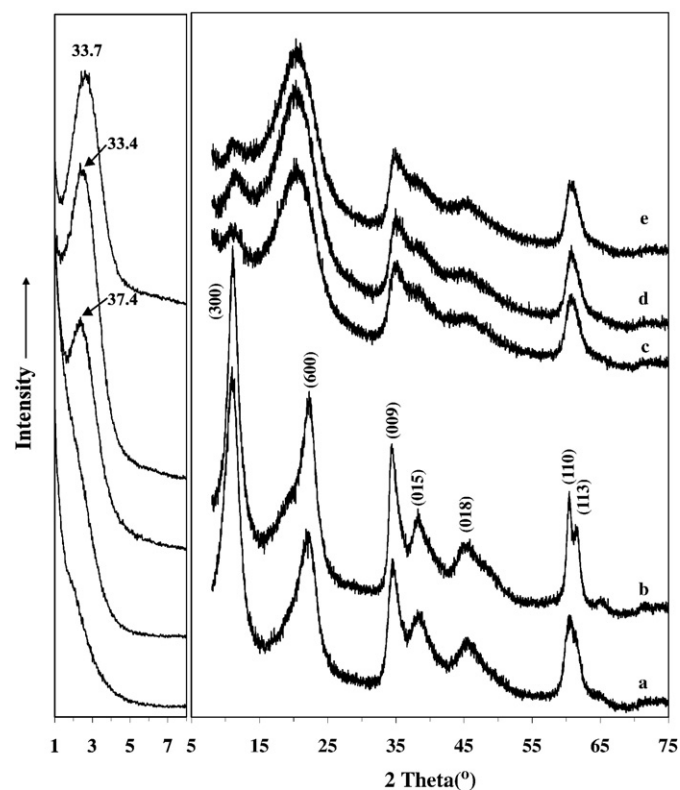

Fig. 1. The XRD patterns of grafted LDHs (range 1–10° and 8–75°): a. LDH-Sil$_{2.5}$, b. LDH-Sil$_5$, c. LDH-Sil$_{10}$, d. LDH-Sil$_{15}$ and e. LDH-Sil$_{20}$.

Table 1
The cell parameters of grafted LDHs.

Samples	Cell parameters									
	New (001)		(003)		(006)		(009)		(110)	
	$2\theta/°$	$d/Å$	$2\theta/°$	$d/Å$	$2\theta/°$	$d/Å$	$2\theta/°$	$d/Å$	$2\theta/°$	$d/Å$
LDH-Sil$_{2.5}$	/	/	11.1	8.0	22.0	4.0	34.6	2.6	60.7	1.5
LDH-Sil$_5$	/	/	11.0	8.1	22.5	3.9	34.4	2.6	60.4	1.5
LDH-Sil$_{10}$	2.4	37.4	11.0	8.0	20.9	4.2	34.9	2.6	60.7	1.5
LDH-Sil$_{15}$	2.6	33.4	11.3	7.8	20.2	4.4	34.8	2.6	60.5	1.5
LDH-Sil$_{20}$	2.6	33.7	11.4	7.8	20.5	4.3	35.1	2.6	60.6	1.5

thermobalance (TA, USA). About 50 mg samples were heated in an open platinum crucible between 25 and 1000 °C with a heating ratio of 6 °C min^{-1} under N$_2$ atmosphere (100 ml min^{-1}).

3. Results and discussion

3.1. XRD results

The X-ray diffraction patterns are very powerful for the determination of the structure of layered materials. The d value of the layered materials, which reflects the interlayer arrangements, can be directly calculated from Bragg's Law. With the increase of the surfactant concentration, two different series of reflections were observed (Fig. 1), reflecting two types of frameworks contained in the obtained materials (Table 1).

In the 2θ region from 8 to 75° (Fig. 1), the samples obtained under low SDS concentration (LDH-Sil$_{2.5}$ and LDH-Sil$_5$) showed sharp reflections with high intensity as (003), (006) and (009). Their d_{003} values are 8.0 and 8.1 Å respectively, similar to the CO$_3^{2-}$ interlayered LDHs. This suggests that the sulfate units of SDS were attracted to the outside surface and/or the plate edges of LDH while the alkyl chains point outwards from the surface (denoted as type I). In this case the APTS may have no chance to enter the interlayer space of LDH either. The only possibility for APTS is to anchor on the external surface and the plate edges by condensation with –OH groups of LDH, similar to those found in clay minerals modification (Herrera et al., 2004; Park et al., 2004).

When the content of SDS increased to 0.010 mol, the reflections at low angles were recorded (Fig. 1c, d and e). These reflections may be assigned to the d_{001} of new formed materials, indicating SDS anions entered the interlayer spaces of LDH (denoted as type II), with d values 37.4 (LDH-Sil$_{10}$), 33.4 (LDH-Sil$_{15}$) and 33.7 Å (LDH-Sil$_{20}$), respectively. These d_{001} values are even larger than the sum of the single LDH layer thickness (4.8 Å), the length of SDS anion (17.8 Å) and the length of APTS (7.5 Å) (O'Leary et al., 2002; Park et al., 2005). Usually, the arrangement of interlayered anions can be deduced from the d_{001} value of the resultant materials. Meyn et al. (1990) assumed that the secondary alkanesulfonates existed and all C–C bonds were in
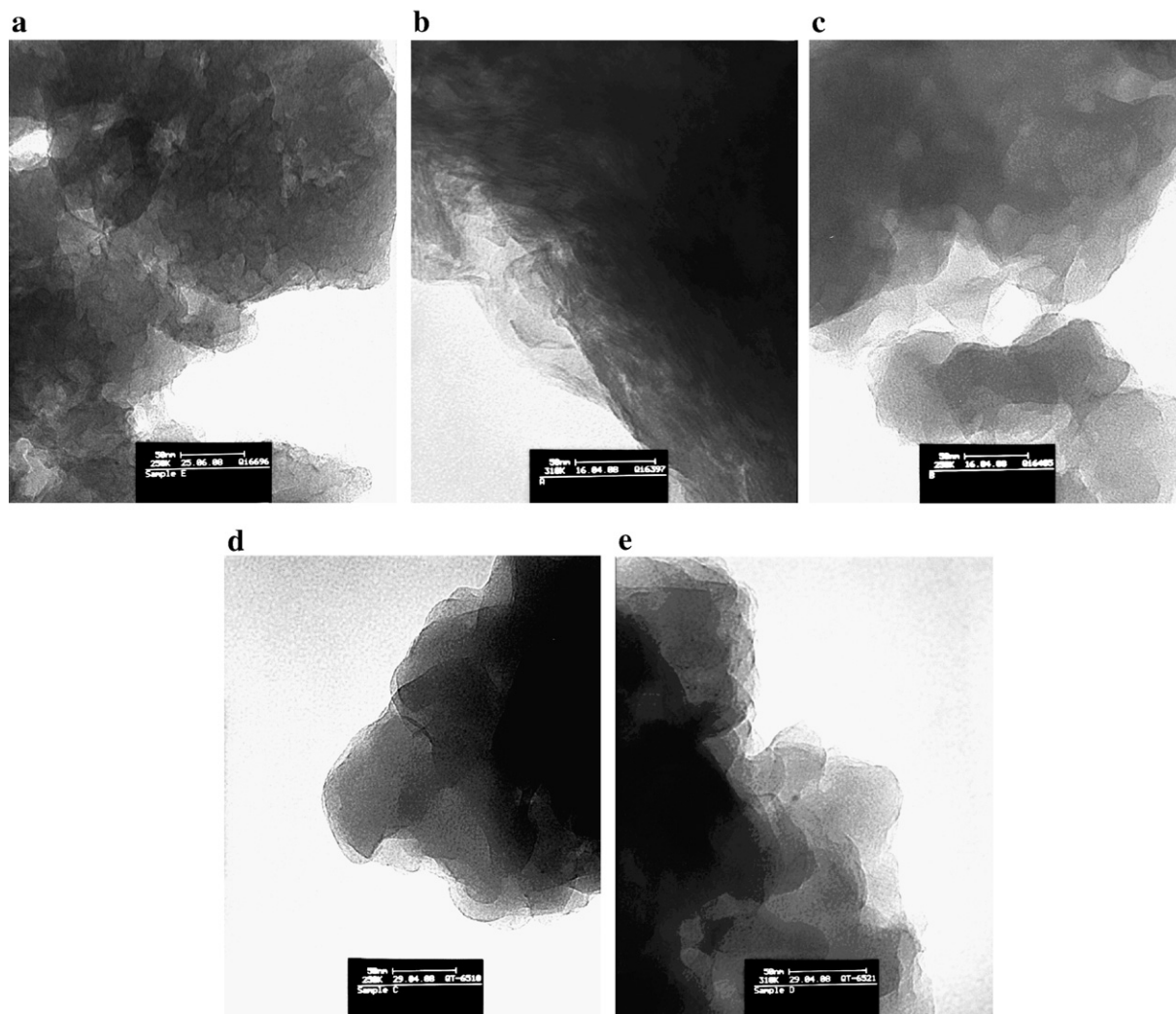

Fig. 2. The TEM images of grafted LDHs: a. LDH-Sil$_{2.5}$, b. LDH-Sil$_5$, c. LDH-Sil$_{10}$, d. LDH-Sil$_{15}$ and e. LDH-Sil$_{20}$.

the trans conformation. Meyn et al. (1993) also reported that when the carbon number was 12 and smaller the arrangement of the anions was likely to be bilayers. When carbon atoms number was 12, the basal spacing is observed as 23.0 Å, while You et al. (2002b) proposed that the monolayer DS⁻ was oriented perpendicular in the interlayer space with the basal spacing about 22.7 Å. Theoretically, a basal spacing of 22.6 and 40.4 Å would be observed for single layer and double layer perpendicular orientation of the DS⁻ between the layers, respectively. In this work, the basal spacings were observed at 33.4–37.4 Å, locating between 22.6 and 40.4 Å. Therefore, the intercalated surfactants are more likely to adopt a paraffin bilayers arrangement model (Lagaly, 1981; You et al., 2002b; He et al., 2004b), similar to those reports about silane modified clay minerals. Because the length of APTS is far smaller than that of SDS, and the organophilicity increases after DS⁻ intercalated (Zhu et al., 2008), the APTS molecules may be easily introduced into the interlayer space and to condensate with the –OH groups on the LDH surfaces.

3.2. Transmission electron microscopy

The silylated LDHs synthesized with different contents of surfactant displayed different morphologies (Fig. 2), corresponding to different stacking modes. The plate-like crystal particles, which are common in the LDHs (Tao et al., 2009), are changed by assistance of surfactant. When the content of SDS was 0.0025 mol (LDH-Sil$_{2.5}$), the particles were formed with random distribution directions. Several layers were bonded to one another to form aggregates, with a thickness of about 2.5 nm. When the surfactant content increased to 0.010 mol (LDH-Sil$_{10}$) and more, such randomly distributed particles were replaced by unified large sheets lying on the grids. The sizes of the sheets increased significantly with the increase of SDS content up to 0.015 mol. At the same time the surface of the grafting products became from smooth to rough. This should be attributed to the condensation between the M–OH (M = Al and Mg) on LDH surface and Si–OH in the hydrolyzed silane. The ribbon-like curled sheets were observed in our earlier work when Na-dodecylsulfonate was used as surface modifier (Tao et al., 2009). However, the ribbon-like curled sheets cannot be found in this study, while SDS was used. This implies that the used surfactants have prominent influence on the morphology of the obtained materials.

The compositions of the samples were obtained by EDX (Table 2). In order to obtain the reliable results, the particles with similar size and thickness were chosen for EDX analysis. As shown in Table 2, the contents of Si are relatively low in type I samples and increases from LDH-Sil$_{10}$ to LDH-Sil$_{15}$, but decreases from LDH-Sil$_{15}$ to LDH-Sil$_{20}$. This may be resulted from the influence of the silane, in which SDS plays a double-edged role in grafting progress. On one hand, SDS bonded on the surface of LDH changes its surface property towards organophilicity, facilitating to introduce the APTS onto LDHs and condensate with the –OH groups located at outside surface and broken edges. On the other hand, when the content of loaded SDS became high, the SDS would cover most available –OH in priority and there would be only limited –OH left for bonding with APTS. This presumption is in accordance with the Si content changes in both type I and II samples.

Table 2
The EDX results of grafted LDHs.

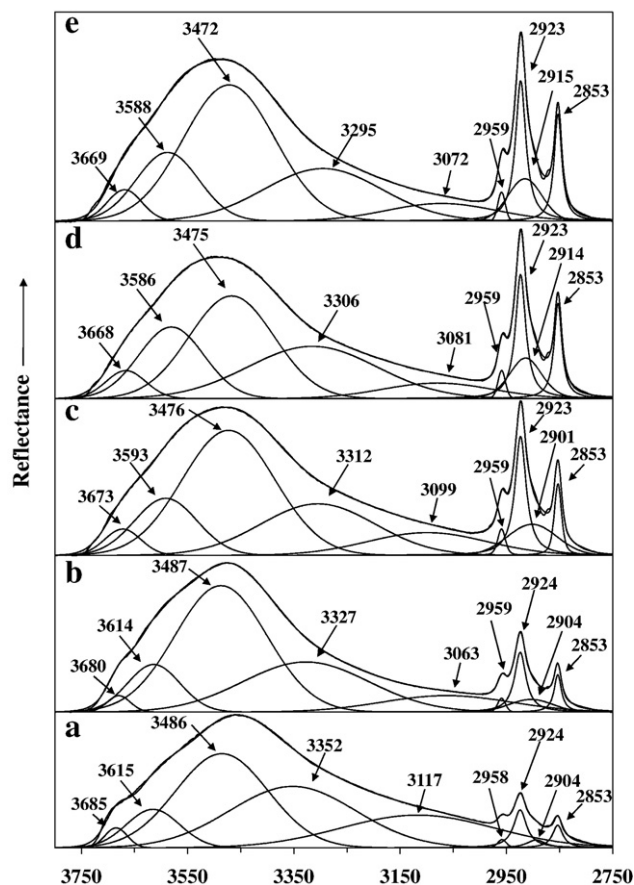| Atomic %					
Samples	Elements				
	Mg	Al	Si	S	Mg/Al/Si/S
LDH-Sil$_{2.5}$	23.57	7.19	1.79	1.42	3.28:1:0.25:0.20
LDH-Sil$_5$	42.36	11.93	1.51	1.78	3.55:1:0.13:0.15
LDH-Sil$_{10}$	20.19	6.36	1.58	3.01	3.17:1:0.25:0.47
LDH-Sil$_{15}$	18.45	6.28	1.87	5.60	2.94:1:0.30:0.89
LDH-Sil$_{20}$	19.02	6.47	1.62	5.00	2.94:1:0.25:0.77

Fig. 3. The FTIR spectra of the grafted LDHs in the 3750–2750 cm⁻¹ region: a. LDH-Sil$_{2.5}$, b. LDH-Sil$_5$, c. LDH-Sil$_{10}$, d. LDH-Sil$_{15}$ and e. LDH-Sil$_{20}$.

In LDH-Sil$_5$, the SDS was rather higher than in LDH-Sil$_{2.5}$ but not enough for exchanging with interlayer CO_3^{2-} and entering interlayer space. Therefore, most –OH groups on outside surface were bonded by SDS, only a small amount left for condensation with APTS. Similarly, after intercalation (type II), the SDS facilitated more APTS to approach to both inside and outside surfaces of LDH. However, when SDS reached a high level as in LDH-Sil$_{20}$, the loaded SDS would hinder the entrance of silane, resulting in a decrease of Si content.

3.3. Infrared spectroscopy

The FTIR spectra of silane grafted LDHs with different contents of SDS were presented in Figs. 3–5, and the band details were summarized in Table 3. The bands corresponding to LDHs (Fig. S1) were usually found at around 3063–3685 (–OH stretching mode), 1630 (–OH bending mode), 1362 (CO_3^{2-}) and below 600 cm⁻¹ (M–OH). The bands corresponding to SDS were also observed, such as C–H stretching and bending (2959–2853 cm⁻¹, and 1468 cm⁻¹), –OSO$_3^-$ stretching and bending (1200, 1061 and 720 cm⁻¹). APTS brought a serial of bands due to –NH$_2$ and Si–O in the region of 1400–1600 cm⁻¹ (Fig. 4), 950–1100 cm⁻¹ (Fig. 5) and 800–500 cm⁻¹ (not shown) with some bands overlapped with those of SDS. In our previous work, the band component analysis was taken to the FTIR spectra of silane grafted samples which showed a neoformative band at about 996 cm⁻¹ (Tao et al., 2009) attributed to the Si–O–M generated from the condensation between Si–OH and –OH of LDHs surface. Similarly, this kind of bands can also be found in this study, which strongly proved that APTS has successfully been grafted onto LDH.

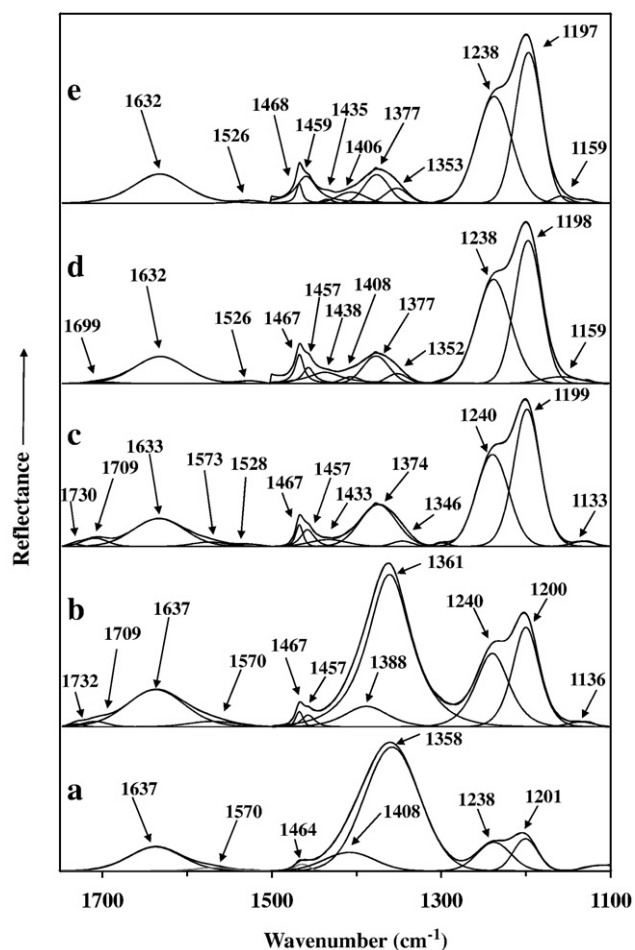With the increase of the SDS content, the grafted materials showed differences in the FTIR spectra, such as the bands of CO_3^{2-} that can be

Fig. 4. The FTIR spectra of the grafted LDHs in the 1750–1100 cm^{-1} region: a. LDH-Sil$_{2.5}$, b. LDH-Sil$_5$, c. LDH-Sil$_{10}$, d. LDH-Sil$_{15}$ and e. LDH-Sil$_{20}$.

covalent bonds between silane and LDH were formed. The bounded silane would occupy the surface (type I) and interlayer space (type II) of LDH hindering the surfactants to have a regular arrangement. The Si–O related band shift showed in a tendency paralleling with their contents as tested by EDX results. Most of these bands shifted to higher wavenumber when compared with that in pure APTS and the explanation is the same as discussed in the arrangement of –CH$_2$.

3.4. Thermal analysis

The thermal analysis was measured to provide the further evidences of the different stacking modes of the grafted products. The TG curves of all grafted samples were shown in Fig. 6. The corresponding differential thermogravimetric analysis profiles were also shown for comparison. The typical LDH showed three mass loss steps (Tao et al., 2009). The first stage was from 31 to 213 °C with the total mass loss of 12.6%, attributed to the loss of adsorbed water, interlayer water and CO$_3^{2-}$ absorbed on the surface. The dehydroxylation stage and partial loss of CO$_3^{2-}$ began at 213 °C and ends at 400 °C, with a mass loss of 21.7%. The last stage occurred from 400 to 690 °C with a mass loss of 11.9 %, due to the complete loss of the interlayer anions to form layered double oxides (LDO). The total mass loss observed was about 46.1% (Fig. S2).

The grafted samples showed significant differences with the pure LDH due to both SDS and APTS (Fig. 6b–f). These differences lay in three main aspects. Firstly, the mass loss due to the interlayer water
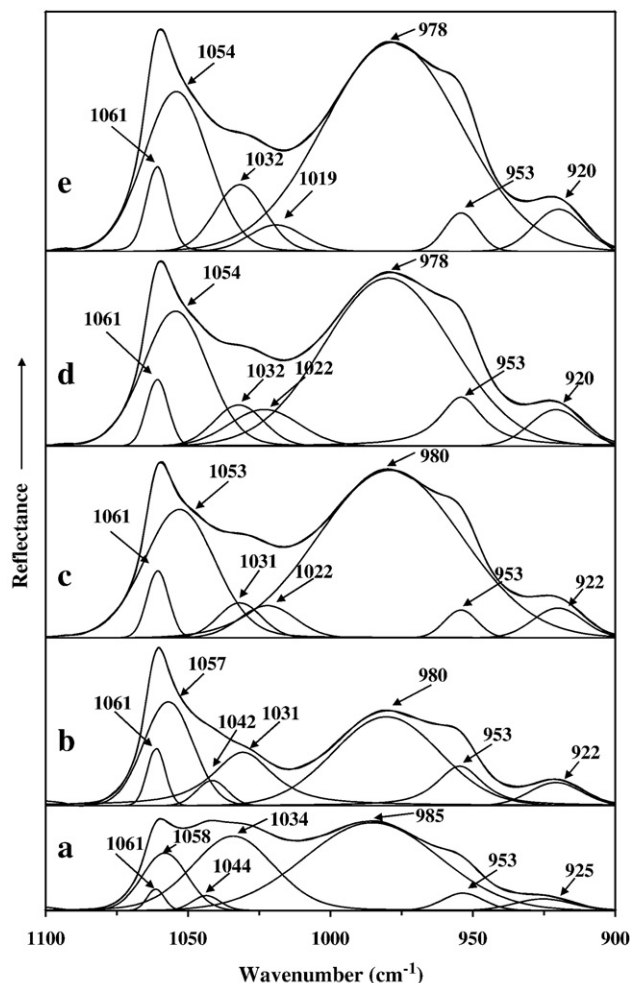

Fig. 5. The FTIR spectra of the grafted LDHs in the 1100–900 cm^{-1} region: a. LDH-Sil$_{2.5}$, b. LDH-Sil$_5$, c. LDH-Sil$_{10}$, d. LDH-Sil$_{15}$ and e. LDH-Sil$_{20}$.

found in the low content of SDS samples become very weak and finally were replaced by SDS related bands (Fig. 4). The bands due to the M–OH and water shifted to lower wavenumber (Fig. 3), the bands due to the stretching mode of –CH$_2$ shifted to higher wavenumber when compared with those in SDS (Fig. 3 and Table 3) and the wavenumber of Si–O related bands changed in a zigzag tendency (Fig. 5). In type I materials, the antisymmetric stretching mode of the interlayered CO$_3^{2-}$ can be clearly observed at about 1360 cm^{-1} with high intensity (Fig. 4a, b). However, when the content of SDS increased (type II, Fig. 4c–e), this band got very weak and was replaced by –CH$_2$ wagging vibrations (1375 cm^{-1}). This indicated that at high content, SDS anions exchanged with the CO$_3^{2-}$ and enter the interlayer spaces of LDHs. In both type I and II materials, the –OH related bands obviously shifted to lower wavenumber. In the previous study, we evidenced that dodecylsulfonate anions interlayered LDHs can change the surface property from hydrophilicity to hydrophobicity by the M–OH related bands shift to higher wavenumbers (Zhu et al., 2008; Tao et al., 2009). So, it is presumed that the grafting reaction takes a significant influence on the vibration wavenumber shift of M–OH vibration to a lower wavenumber. The frequencies of the antisymmetric and symmetric –CH$_2$ stretching vibration bands are sensitive to the conformation of the intercalated alky chains within the layered materials (He et al., 2004a). In all samples, the antisymmetric and symmetric –CH$_2$ stretching bands located at higher wavenumber than that in SDS (Fig. 3 and Table 3), indicating that the conformation of the alkyl chain of the surfactant changes from all-trans to gauche. This gives an important evidence for the successful grafting of the silane onto the LDH. When silane grafted onto LDH surfaces, strong

Table 3
Assignments of the FTIR bands of grafted LDHs with different content of SDS.

LDH	SDS	APTS	Grafted LDHs with different content of SDS (mol)					Assignment
			0.0025	0.0050	0.0010	0.0015	0.0020	
3670, 3606	3461		3685, 3615	3680, 3614	3673, 3593	3668, 3586	3669, 3588	M–OH stretching
3466	3461		3486	3487	3476	3475	3472	Absorbed H_2O
3314			3352	3327	3312	3306	3295	H-bonds between –OH and H_2O
3073			3117	3063	3099	3081	3072	The bridge bond between H_2O and anions
	2955–2851	2975–2885	2958–2853	2959–2853	2959–2853	2959–2853	2959–2853	–CH_3 and CH_2 anti- and symmetric stretching
1636			1637	1637	1633	1632	1632	H_2O bending
			1570	1570	1573			–NH_2 scissoring
	1467		1464	1467	1526, 1467	1526, 1467	1526, 1468	–NH_2 deformation
		1454, 1443		1457	1457, 1433	1457, 1438	1459, 1435	–CH_2 scissoring and Si–CH_2 scissoring
	1366	1365			1388	1378	1378	–CH_2– wagging
1360			1358	1361	1346	1352	1353	CO_3^{2-} antisymmetric stretching (v_3)
	1250		1238	1240	1240	1238	1238	–CH_3 scissoring and OSO_3^- antisymmetric stretching
	1068		1204, 1061	1200, 1061	1199, 1061	1198, 1061	1198, 1061	–OSO_3^- antisymmetric and symmetric stretching
		1080	1058	1057	1053	1054	1054	Si–O stretching
		1070	1044	1042	1031	1032	1032	Si–O–C asymmetric stretching
			1034	1031	1022	1022	1019	S–O in-plane stretching
		968	985	980	980	978	978	Si–O–M stretching
			953	953	953	953	953	Si–O stretching
	920		925	922	922	920	920	O–H deformation of surface hydroxyl groups
827			826	825	825	826	825	CO_3^{2-} v_2 stretching
		793			800	806	807	Si–O symmetric stretching
	720		720	721	720	719	723	O–S–O bending
			657, 615	654, 613	658, 621	650, 622	655, 621	Si–O–M deformation
576			583	578	581	571	589, 579	Si–O–M bending

decreased. This implies that the modification of LDH with SDS results in an affinity change of LDH plate surface from hydrophilicity to hydrophobicity as discussed in previous works (Zhu et al., 2008), leading to a decrease of sorbed water within LDH. Also, the limited residual water would be consumed during silylation reaction. Secondly, the stages corresponding to dehydroxylation and anion volatilization were changed with the existence patterns of SDS. Similar to the XRD results, the grafted samples can be divided to similar two types. In type I (Fig. 6b and c), the SDS anions were only absorbed on the outside surface and plate edges of LDH. In this case, the mass loss stages from about 150 to 400 °C were similar with those of pure LDH. The difference was that the LDH-Sil$_5$ showed a clear loss of absorbed SDS at a temperature range from 134 to 180 °C and the alkyl group loss stage was overlapped with that of the dehydroxylation. The mass loss in 415–551 °C in LDH-Sil$_{2.5}$ and 433-538 °C in LDH-Sil$_5$ was ascribed to volatilization of interlayer CO_3^{2-} and loss of the residual –OH in LDH. The less mass loss indicated the interlayer CO_3^{2-} was partly exchanged by SDS during the grafting process. When the content of SDS increases to 0.010 mol and above (Fig. 6e–g), the interlayer space of the resultant materials is dominated by SDS (type II). These materials typically lose alkyl chains at around 210 °C as can be observed in TG curve (Fig. 6a). The dehydroxylation mass loss of the three samples of type II were about 24.9% (269–410 °C), 23.8% (270–426 °C) and 24.6% (275–430 °C), respectively. The less mass loss of –OH in LDH-Sil$_{15}$ agreed well with the more Si content obtained from EDX test (Table 2), indicating the –OH consumption by the condensation between APTS and the hydroxyl groups on LDH plates to form Si–O–M (M = Mg^{2+} or Al^{3+}) as evidenced by the FTIR spectral changes (Zhu et al., 2008).

The volatilization of –OSO_3^- and further dehydroxylation happened when temperature come up to about 550 °C to form SO_2 and layered double oxides (LDO) mixtures. These procedures were evidenced in details by Clearfield et al. (1991) through the IR spectra of samples after calcinations to detect the evolved gases. In this temperature range, different from pure LDH and type I materials, type II materials present extra mass losses at beyond 750 °C (Fig. 6d–f). These mass losses should be attributed to the further dehydroxylation to form MgO, Al_2O_3, SiO_2, SO_3 and H_2O (Clearfield et al., 1991). This suggests

that the obtained materials with much higher thermal stability are generated by grafting reaction with higher content of SDS and APTS.

4. Conclusions

The APTS grafted LDHs have been synthesized using an in-situ coprecipitation method. The mixed metal nitrates and alkali solution were coprecipitated together with silane and surfactant. The SDS played a very important influence on the structure and thermal properties of the obtained materials. In the materials synthesized with low surfactant content, SDS and APTS were bonded to the outside surface and plate edges of LDHs. In the other type (synthesized with high surfactant content), the SDS and APTS were combined with both inside and outside surfaces of LDHs. As shown by TEM images, the surfaces of the silane grafted LDHs become rough due to the APTS condensation with the plates of LDHs. The bands related to –NH_2 and Si–O in FTIR spectra confirmed the success of grafting APTS to the surface of LDHs. The conformation change of the intercalated surfactant from all-trans to gauche with the increased content of SDS provided a complementary support for the success of the silane grafting. Meanwhile, different concentrations of –OH group and interlayer water molecules in different types of silane grafted LDH as indicated by the TG curves suggested the –OH consumption during the condensation reaction between Si–OH in hydrolyzed silane and –OH on LDH surface. The silane grafted products showed higher thermal stability than pure LDHs. These nanomaterials are of potential applications including clay-based nanocomposites, adsorbents for removal of organic contaminants from water and flame retardant materials.

Fig. 6. The TG curve of the grafted LDHs: a. SDS, b. LDH-Sil$_{2.5}$, c. LDH-Sil$_5$, d. LDH-Sil$_{10}$, e. LDH-Sil$_{15}$ and f. LDH-Sil$_{20}$.

Appendix A. Supplementary data

Supplementary data associated with this article can be found, in the online version, at doi:10.1016/j.clay.2009.06.007.

References

Adachi-Pagano, M., Forano, C., Besse, J.P., 2000. Delamination of layered double hydroxides by use of surfactants. Chem. Commun. 1, 91–92.

Angloher, S., Kecht, J., Bein, T., 2007. Metal–organic modification of periodic mesoporous silica: multiply bonded systems. Chem. Mater. 19 (23), 5797–5802.

Cavani, F., Trifiro, F., Vaccari, A., 1991. Hydrotalcite-type anionic clays: preparation, properties and applications. Catal. Today 11 (2), 173–301.

Choudary, B.M., Chowdari, N.S., Jyothi, K., Kantam, M.L., 2002. Catalytic asymmetric dihydroxylation of olefins with reusable OsO$_4^{2-}$ on ion-exchangers: the scope and reactivity using various cooxidants. J. Am. Chem. Soc. 124 (19), 5341–5349.

Clearfield, A., Kieke, M., Kwan, J., Colon, J.L., Wang, R.C., 1991. Intercalation of dodecyl sulfate into layered double hydroxides. J. Incl. Phenom. Macrocycl. Chem. 11 (4), 361–378.

Dimotakis, E.D., Pinnavaia, T.J., 1990. New route to layered double hydroxides intercalated by organic anions: precursors to polyoxometalate-pillared derivatives. Inorg. Chem. 29 (13), 2393–2394.

Domingo, C., Loste, E., Fraile, J., 2006. Grafting of trialkoxysilane on the surface of nanoparticles by conventional wet alcoholic and supercritical carbon dioxide deposition methods. J. Supercrit. Fluids 37 (1), 72–86.

Drezdzon, M.A., 1988. Synthesis of isopolymetalate-pillared hydrotalcite via organic-anion-pillared precursors. Inorg. Chem. 27 (25), 4628–4632.

He, H., Frost, R.L., Zhu, J., 2004a. Infrared study of HDTMA$^+$ intercalated montmor-illonite. Spectrochim. Acta, A 60 (12), 2853–2859.

He, H.P., Frost, R.L., Deng, F., Zhu, J.X., Wen, X.Y., Yuan, P., 2004b. Conformation of surfactant molecules in the interlayer of montmorillonite studied by ^{13}C MAS NMR. Clay. Clay Miner. 52 (3), 350–356.

Hermosin, M.C., Pavlovic, I., Ulibarri, M.A., Cornejo, J., 1996. Hydrotalcite as sorbent for trinitrophenol: sorption capacity and mechanism. Water Res. 30 (1), 171–177.

Herrera, N.N., Letoffe, J.M., Putaux, J.L., David, L., Bourgeat-Lami, E., 2004. Aqueous dispersions of silane-functionalized laponite clay platelets. A first step toward the elaboration of water-based polymer/clay nanocomposites. Langmuir 20 (5), 1564–1571.

Hutson, N.D., Speakman, S.A., Payzant, E.A., 2004. Structural effects on the high temperature adsorption of CO$_2$ on a synthetic hydrotalcite. Chem. Mater. 16 (21), 4135–4143.

Ingall, M.D.K., Honeyman, C.H., Mercure, J.V., Bianconi, P.A., Kunz, R.R., 1999. Surface functionalization and imaging using monolayers and surface-grafted polymer layers. J. Am. Chem. Soc. 121 (15), 3607–3613.

Lagaly, G., 1981. Characterization of clays by organic compounds. Clay Miner. 16 (1), 1–21.

Lee, H., Dellatore, S.M., Miller, W.M., Messersmith, P.B., 2007. Mussel-inspired surface chemistry for multifunctional coatings. Science 318 (5849), 426–430.

Leroux, F., Adachi-Pagano, M., Intissar, M., Chauviere, S., Forano, C., Besse, J.P., 2001. Delamination and restacking of layered double hydroxides. J. Mater. Chem. 11 (1), 105–112.

Li, C., Wang, G., Evans, D.G., Duan, X., 2004. Incorporation of rare-earth ions in Mg–Al layered double hydroxides: intercalation with an [Eu(EDTA)]$^-$ chelate. J. Solid State Chem. 177 (12), 4569–4575.

Meyn, M., Beneke, K., Lagaly, G., 1990. Anion-exchange reactions of layered double hydroxides. Inorg. Chem. 29 (26), 5201–5207.

Meyn, M., Beneke, K., Lagaly, G., 1993. Anion-exchange reactions of hydroxy double salts. Inorg. Chem. 32 (7), 1209–1215.

O'Leary, S., O'Hare, D., Seeley, G., 2002. Delamination of layered double hydroxides in polar monomers: new LDH-acrylate nanocomposites. Chem. Commun. 14, 1506–1507.

Oh, S., Kang, T., Kim, H., Moon, J., Hong, S., Yi, J., 2007. Preparation of novel ceramic membranes modified by mesoporous silica with 3-aminopropyltriethoxysilane (APTES) and its application to Cu^{2+} separation in the aqueous phase. J. Membr. Sci. 301 (1–2), 118–125.

Park, M., Shim, I.-K., Jung, E.-Y., Choy, J.-H., 2004. Modification of external surface of laponite by silane grafting. J. Phys. Chem. Solids 65 (2–3), 499–501.

Park, A.Y., Kwon, H., Woo, A.J., Kim, S.J., 2005. Layered double hydroxide surface modified with (3-aminopropyl)triethoxysilane by covalent bonding. Adv. Mater. 17 (1), 106–109.

Tao, Q., He, H.P., Frost, R.L., Yuan, P., Zhu, J.X., 2009. Nanomaterials based upon silylated layered double hydroxides. Appl. Surf. Sci. 255 (7), 4334–4340.

Wypych, F., Bail, A., Halma, M., Nakagaki, S., 2005. Immobilization of iron (III) porphyrins on exfoliated Mg–Al layered double hydroxide, grafted with (3-aminopropyl)triethoxysilane. J. Catal. 234 (2), 431–437.

Yeon, Y.R., Park, Y.J., Lee, J.S., Park, J.W., Kang, S.G., Jun, C.H., 2008. Sc(OTf)$_3$-mediated silylation of hydroxy functional groups on a solid surface: A catalytic grafting method operating at room temperature. Angew. Chem., Int. Edit. 47 (1), 109–112.

You, Y.W., Zhao, H.T., Vance, G.F., 2002a. Hybrid organic–inorganic derivatives of layered double hydroxides and dodecylbenzenesulfonate: preparation and adsorption characteristics. J. Mater. Chem. 12, 907–912.

You, Y.W., Zhao, H.T., Vance, G.F., 2002b. Surfactant-enhanced adsorption of organic compounds by layered double hydroxides. Colloid. Surf., A 205 (3), 161–172.

Zhu, J.X., Yuan, P., He, H.P., Frost, R., Tao, Q., Shen, W., Bostrom, T., 2008. In situ synthesis of surfactant/silane-modified hydrotalcites. J. Colloid Interface Sci. 319 (2), 498–504.